Molecular quantum wakes in the hydrodynamic plasma waveguide in air

Jian Wu,[1] Hua Cai,[1] H. M. Milchberg,[2] and Heping Zeng[1,*]

[1]*State Key Laboratory of Precision Spectroscopy, East China Normal University, Shanghai 200062, China*

[2]*Institute for Research in Electronics and Applied Physics, University of Maryland, College Park, Maryland 20742, USA*

We demonstrate a modulated plasma guiding effect from the molecular alignment wakes in the hydrodynamic plasma waveguide. A properly time-delayed laser pulse can be spatially confined by the hydrodynamic expansion induced plasma waveguide of an advancing femtosecond laser pulse. The spatial confinement can be further strengthened or weakened by following the quantum wakes of the impulsively excited rotational wave packets of the molecules in the plasma waveguide.

I. INTRODUCTION

Advancements in laser technology have greatly expanded the high-peak-intensity range of ultrashort lasers, and many important applications require tightly guided high-peak intensities of long interaction distances. Guiding of intense pulses has been demonstrated in plasma waveguides through discharges in hollow capillaries [1,2], or hydrodynamic plasma waveguides through radial expansion of the laser-induced plasma columns [3,4]. Tight guiding in plasma waveguides provides a solution to avoiding detrimental defocusing caused by further photon ionization and could reach an ultrahigh intensity tolerance up to 5×10^{17} W/cm^2 [4], but it is hardly applicable to neutral gases. On the other hand, Kerr self-focusing could be used to counterbalance the ionization-induced plasma defocusing in neutral media, resulting in self-channeled filaments for self-guiding femtosecond (fs) laser pulses of modest intensities [5–8]. Interestingly, such self-guiding in molecular gases exhibits additional cross-(de)focusing arose from molecular alignment wakes [9–13]. After filamentation, radial expansion of the plasma could also establish hydrodynamic plasma waveguides, which should coexist with molecular wakes as long as the molecules are not totally ionized. However, the influence of molecular wakes on plasma guiding has not yet been investigated at all, and it may provide us with an essential and robust method to control the plasma waveguide in molecular gases.

In this paper, we investigate the effect of molecular alignment wakes on the fs laser pulse propagation in a hydrodynamic plasma waveguide. In a pump-probe experiment with a fs laser pulse propagating in air, a hydrodynamic plasma waveguide was induced through radial plasma expansion of the pump filament, and plasma guiding was observed for a time-delayed probe pulse. The guiding effect could be strengthened (weakened) by cross-focusing (defocusing) from the parallel (perpendicular) molecular alignment revivals, confirming that quantum wakes of the preexcited molecular rotational wave packets could be used to control hydrodynamic plasma guiding of ultrashort laser pulses.

The optical guiding of the probe laser pulse by the plasma waveguide [14] is in principle based on the refractive index variation $\delta n_{plas} \sim -0.5 N_e/N_{cr}$ across the plasma radial

profile, where N_e is the electron density and N_{cr} ($\sim 6.9 \times 10^{21}$ cm^{-3} for 400 nm) is the critical density. A laser-induced plasma column initially exhibits a radial density distribution dependent upon the laser spatial profile with the plasma density peak on axis, which expands outward owing to the radially inward-directed pressure gradient [3], resulting in a plasma density and spatial profile varying with the time delay. At proper time delays, the plasma is expanded to have a lower density on axis, corresponding to a higher refractive index on axis. Accordingly, the expanded plasma column functions as an optical waveguide and is especially useful for guiding intense laser pulses. Most of the recent pertinent work used high-energy pulses to generate high-density plasma for a hydrodynamic plasma waveguide [3,4]. As we will show here, that plasma within the fs filament of modest plasma density also experiences hydrodynamic plasma expansion after filamentation and forms the corresponding plasma waveguide at proper delays. In air, the residual neutral molecules in the pump filament are aligned through impulsive rotational Raman excitation. The molecular alignment and its revivals change the refractive index and hence can be used to control the plasma guiding. Depending on the relative alignment of the molecules with respect to field polarization, the molecular effect either cooperates with or opposes the effect of the plasma waveguide, as schematically shown in Fig. 1(a).

II. EXPERIMENTAL SETUP

We carried out the experiments with a 1 kHz regenerative Ti:sapphire laser amplifier of 35 fs pulse duration at 800 nm. The output pulse was split into two pulses. The intense part was used as the pump to generate a plasma column in air, and the weak one was frequency-doubled to generate a second-harmonic (SH) probe pulse of ~ 10 μJ pulse energy by using a 200-μm-thick type-I beta barium borate (BBO) crystal. By using a half-wave plate at 400 nm, the probe polarization was rotated parallel to the pump one. Before collinear combination with a dichromatic mirror, the pump and probe pulses were focused with two convex lenses of the same focal length ($f = 40$ cm), while the probe focus was intentionally located ~ 1.0 cm after the beginning of the pump column in order to check the plasma guiding effects. By blocking the intense pump pulse, we measured the focus radius of the weak probe pulse to be $w_0 \sim 23$ μm at $1/e^2$. The pump-probe delay was controlled with a motorized translation

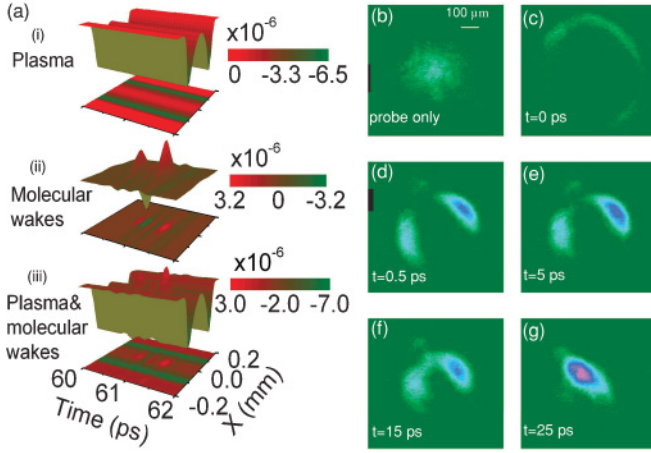*Corresponding author: hpzeng@phy.ecnu.edu.cn

FIG. 1. (Color online) (a) Refractive index changes induced by the plasma (i), molecular wakes (ii), and simultaneous plasma and molecular wakes (iii). (b)–(g) Measured two-dimensional spatial profiles of the SH pulse at various delays.

stage in the pump arm. To produce a stable plasma column of a single core, the laser pulse was tuned to $\sim$130 fs in duration by adjusting the compressor grating separation in the laser system. With a pump pulse energy of $\sim$5.5 mJ, a plasma column of $\sim$3 cm in length was generated in air. The plasma guiding of the probe pulse was then studied directly by imaging its spatial profiles at the end of the plasma column with a $4f$ imaging system and comparing the spatial profile changes at various pump-probe delays. We collected only the probe pulse into a charge-coupled device (CCD) by using several dichromatic mirrors of high reflection at 400 nm and high transmission at 800 nm. Rather than free-diffraction propagation, the $4f$ imaging system provides us the real spatial profile of the laser pulse at the end of plasma column.

III. RESULTS AND DISCUSSIONS

A. Hydrodynamic plasma waveguide

Figure 1(b) shows the measured probe beam profile in the absence of the plasma column. For probe injection at the pump filamentation [Fig. 1(c)], the SH probe pulse was spatially diffracted to form a ring structure with a dark hole at the beam center, consistent with probe beam diffraction from a plasma with the plasma density peak on axis. As shown in Figs. 1(d)–1(f), the ring radius became smaller and smaller as the filament plasma expanded outward at later delays, implying that the outward refraction reduced owing to the reduced electron density gradient near the beam center as the plasma column expanded. Eventually, the SH probe beam was confined into a single mode, as shown in Fig. 1(g), with the typical beam radius of $w_0 \sim 90$ μm at a delay of $\sim$25 ps.

We define a probe-beam-mode figure of merit (FOM) by integrating the SH intensity of a fixed small area around the image beam center recorded on the CCD, corresponding to a beam central core of $w_0 \sim 90$ μm at the exit of the plasma column. This allowed us to consider the probe intensity change around the central spatial profile, and no high-order spatial modes were involved in the FOM calculation. The FOMs at different pump-probe delays could reflect the spatial
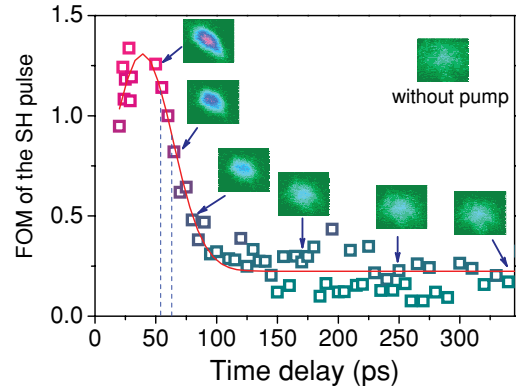

FIG. 2. (Color online) Measured FOM of the SH pulse vs time delay. Inset: Beam profile of probe pulse without pump pulse.

confinement of the probe pulse in the plasma guiding with respect to the outward refraction. Figure 2 shows the FOM of the probe versus the pump-probe delay. The FOM increased initially with the delay up to a maximum at $\sim$39 ps. After this point, the FOM quickly declined with the delay, reaching 50% of the maximum at the delay of $\sim$72 ps, and beyond $\sim$100 ps to an approximately constant level. The spatial profiles of the probe pulse at selected delays are also shown in Fig. 2.

The results of Figs. 1 and 2 allow us to interpret the FOM as a nominal degree of plasma confinement of the probe beam. The trapping and guiding of the probe pulse by the expanded plasma waveguide was started around $\sim$25 ps, where the probe-beam mode has nearly minimum radius and maximum intensity. Here, the trapping of the time-delayed probe pulse was induced by the plasma waveguide with an on-axis plasma density minimum, which became negligibly weak for time delay $t > 100$ ps, as shown in Fig. 2. There the modes had bigger diameters and lower peak intensities, consistent with the plasma-free probe-beam image shown as the inset of Fig. 2. We can estimate the depth of the electron density depression responsible for the guiding using $\Delta N_e = (r_e \pi w_0^2)^{-1}$, where w_0 is the Gaussian beam $1/e^2$ intensity radius, ΔN_e is the electron density difference between $r = 0$ and $r = w_0$, and $r_e \sim 2.82 \times 10^{-15}$ m is the classical electron radius. For $w_0 \sim 90$ μm in Fig. 1(g), we get $\Delta N_e \sim 1.4 \times 10^{16}$ cm^{-3}. Experimentally, by using on-axis holography [15], the electron density of the plasma was measured to be $\sim$1.8 $\times$ 10^{17} cm^{-3}, indicating that about 0.7% of the room-temperature atmosphere air with an initial density of 2.5×10^{19} cm^{-3} was ionized. The field intensity of the filament was hence estimated to be about 8.3 $\times$ 10^{13} W/cm^2 by considering the photon ionization of the air molecules [16].

B. Molecular alignment in plasma waveguide

Besides the hydrodynamic plasma guiding, the molecular alignment augmented the refractive index variation by $\delta n_{\mathrm{mol}}(r,t) \sim 2\pi (N_{\mathrm{mol}} \Delta \alpha / n_0)$ $[\langle\langle \cos^2 \theta(r,t) \rangle\rangle - 1/3]$ [see Fig. 1(a)(ii)], where, N_{mol} is the number density of the neutral molecules, $\Delta \alpha$ is the polarizability difference between the components parallel and perpendicular to the molecular axis, n_0 is the linear refractive index, $\langle\langle \cos^2 \theta \rangle\rangle$ is the degree of
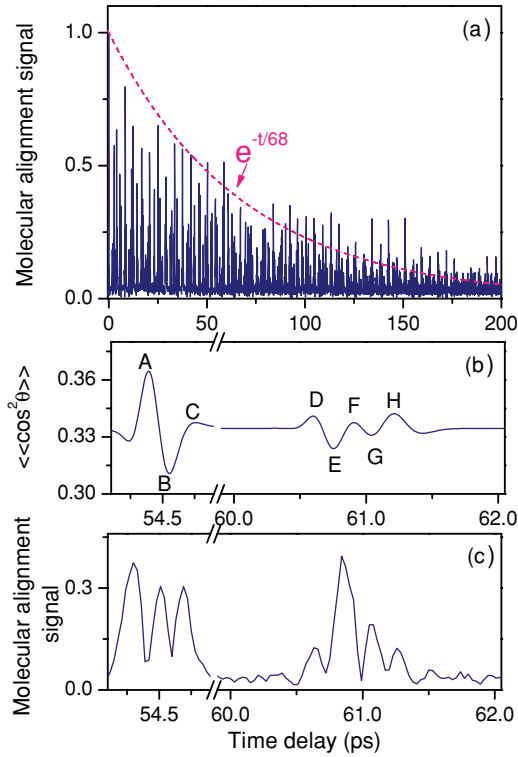
FIG. 3. (Color online) (a) Measured molecular alignment signal $\sim |\langle\langle\cos^2\theta\rangle\rangle - 1/3|^2$, and (b) the calculated $\langle\langle\cos^2\theta\rangle\rangle$ of air. (c) Measured molecular alignment signal of air from 54 to 62 ps.

molecular alignment, and θ is the angle between the field polarization and the molecular axis. For molecular N_2 and O_2 with $\Delta\alpha \sim 1.0$ and 1.15 Å^3 [17], a molecular alignment degree of $\langle\langle\cos^2\theta\rangle\rangle - 1/3 \sim 0.016$ gives a refractive index change of $\delta n_{mol} \sim 2.0 \times 10^{-6}$ and 0.6×10^{-6} at the alignment revivals of N_2 and O_2 in air, respectively. The spatially Gaussian-shaped pump pulse determined the spatial distribution of the molecular alignment degree and refractive index variation, leading to controllable cross focusing or defocusing for parallel ($\langle\langle\cos^2\theta\rangle\rangle - 1/3 > 0$) or perpendicularly ($\langle\langle\cos^2\theta\rangle\rangle - 1/3 < 0$) aligned molecules, respectively.

Figure 3(a) shows the measured molecular alignment signal of the diatomic molecules in air versus the time delay by using the conventional polarization spectroscopy technique [18]. In brief, a linearly polarized weak pulse was noncollinearly crossed with an intense aligning pulse at a small angle in air. The polarization of the weak pulse was set to be 45° with respect to that of the aligning pulse. Since the pre-aligned linear molecules showed different refractive indexes for the field components parallel and perpendicular to the molecular axis, the weak pulse would experience a polarization rotation when its time delay was tuned to match the molecular alignment revival. The polarization rotation of the weak pulse was then detected by a photodiode and analyzed by using a lock-in amplifier after a high-contrast polarizer whose transmission direction was set to be perpendicular to the input polarization of the weak pulse. The measured periodical modulation of the transmitted energy of the weak pulse as a function of its time delay
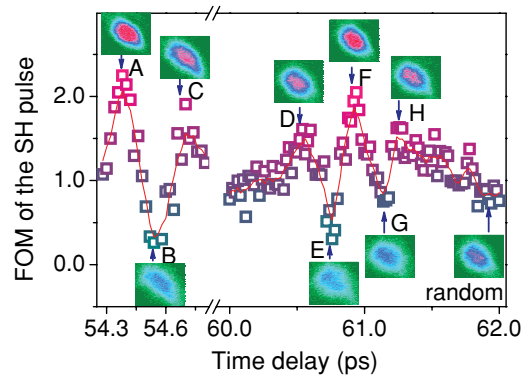

FIG. 4. (Color online) Measured FOM of the SH pulse when its time delay is tuned to match the molecular alignment revivals of the neutral molecules in the hydrodynamic plasma waveguide.

reflected the field-free revivals of the molecular alignment, which was proportional to $\sim |\langle\langle\cos^2\theta\rangle\rangle - 1/3|^2$. Due to the time-dependent decay of the excited rotational wave packets of the molecules, the molecular alignment degree decreased gradually. Meanwhile, the room-temperature molecules slowly diffused away from the interaction region and might also have gradually decreased the measured molecular alignment signal. For the molecular alignment revival with a typical width of a few hundred fs, the plasma expansion and recombination and molecular diffusion was negligibly small. As shown by the fitted red curve, the alignment degree decreased to be $\sim 1/e$ at a time delay of ~ 68 ps after the pump pulse excitation. We hence studied the spatial confinement of the probe pulse around the time delay from 54 to 62 ps to investigate the simultaneous guiding effects of the hydrodynamic plasma waveguide and the molecular wakes [see Fig. 1(a)(iii)]. As marked with dashed lines in Fig. 2, the FOM of the probe pulse decreased from 1.1 to 0.9 when the time delay increased from 54 to 62 ps. We calculated the alignment degree $\langle\langle\cos^2\theta\rangle\rangle$ of air [19] by considering 80% contribution of N_2 and 20% contribution of O_2, as shown in Fig. 3(b). The corresponding molecular alignment signal in this time range measured by using the conventional polarization spectroscopy method is shown in Fig. 3(c).

Figure 4 shows the measured relative spatial confinement of the SH probe pulse when its time delay was tuned to match the molecular alignment revivals in the hydrodynamic plasma waveguide. As expected, the spatial confinement was modulated by following the molecular wakes [10] in the plasma waveguide. The confinement degree was increased or decreased when the time delay of the SH probe pulse was tuned to match the parallel or perpendicular revivals of the molecular alignment, respectively. The absence of this significant change of the FOM of the probe pulse in Fig. 2 was due to the large time step we used where the molecular alignment revival with only a few hundred fs width was not properly matched. As we can see from the two-dimensional spatial profiles of the SH pulse shown in Fig. 4, for parallel alignment revivals at delays A, C, D, F, and G, the SH pulse was tightly confined with intense cores as compared with those for the perpendicular alignment revivals at delays B, E, and G which were also much less intense than that of random orientation. These enhanced and weakened spatial confinement of the
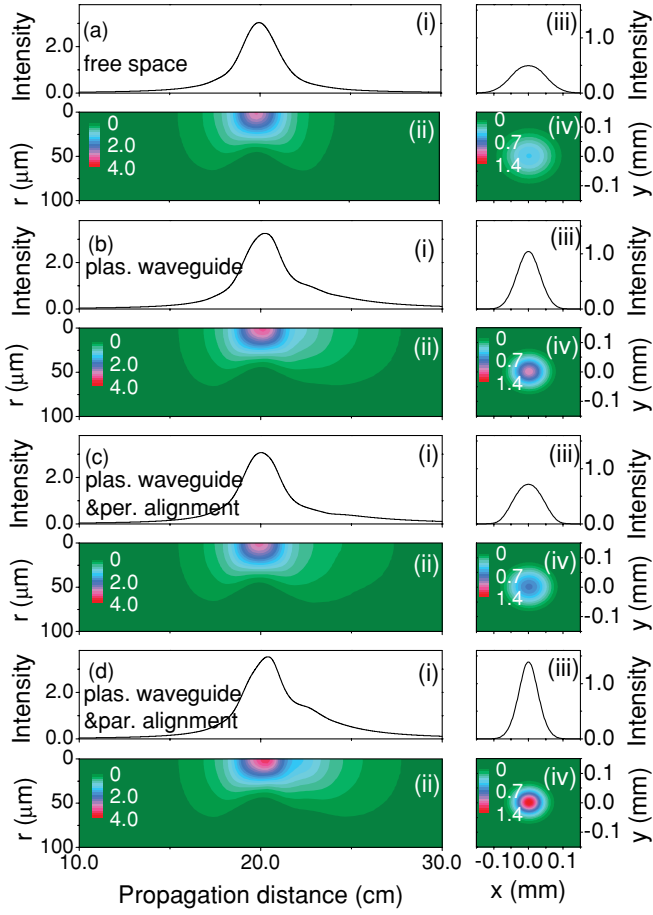
FIG. 5. (Color online) Simulated propagation dynamics of the SH pulse (a) in free space, and (b–d) in plasma waveguide. The SH pulse is tuned to match the (c) perpendicular and (d) parallel revivals of the molecular alignment. (i) and (ii) show the on-axis field intensity and the spatial profile of the SH pulse vs propagation distance, and (iv) and (iii) show the two-dimensional spatial profile and the lineout (through the beam center) of the SH pulse at the end of the plasma waveguide, respectively.

SH pulse at the periodic molecular alignment revivals clearly indicate influence of the molecular wakes on the plasma waveguide.

C. Numerical simulation

Figure 5 shows the numerically simulated dynamics of the SH beam guiding in a $\sim$3 cm-long plasma waveguide. For probe pulses of weak intensities, only the linear spatial diffraction and refractive index modulations induced by the plasma and molecular alignment revivals were taken into account in the propagation equation [10,12,19]:

$$\frac{\partial E_{\text{probe}}}{\partial z} = \frac{0.5i}{k_0}\left(\frac{\partial^2}{\partial r^2} + \frac{1}{r}\frac{\partial}{\partial r}\right)E_{\text{probe}}$$
$$+ ik_0(\delta n_{\text{mol}} + \delta n_{\text{plas}})E_{\text{probe}}.$$

Here, a parabolic transverse plasma density profile [14] is assumed as

$$N_e(r) = N_e(0) + N_{\text{cr}}(r/a)^2$$

for $r < r_m$, and

$$N_e(r) = N_e(r_m)\exp[-(r - r_m)^2/rs^2]$$

for $r > r_m$, where $N_e(0) = 1 \times 10^{16}$ cm^{-3}, $r_m = 100$ μm, $r_s = 20$ μm, and $a = 2 \times 10^4$ μm. The assumption of a parabolic plasma profile applies to the plasma column after radial hydrodynamic expansion. In this situation, a radial plasma sound wave propagates at a speed faster than the speed of sound in the ambient neutral gas, resulting in a radially symmetric shock wave with an electron density minimum on axis. Actually, for radial distances close to the optical axis, assuming a parabolic profile is a good approximation. The molecular alignment degree is set to be $\langle\langle\cos^2\theta\rangle\rangle - 1/3 \sim \pm 0.018$, which gives a refractive index change of $\delta n_{\text{mol}} \sim \pm 2.2 \times 10^{-6}$ for N$_2$ in air. Here, the positive or negative change of the refractive index generally stands for the molecules that are parallel or perpendicular to the probe pulse polarization rather than a specific time delay. In comparison with the case of free propagation shown in Fig. 5(a), the SH beam was guided and spatially confined at the end of the plasma waveguide as shown in Fig. 5(b), which were further modulated when its time delay was tuned to match the perpendicular and parallel revivals of the molecular alignment as shown in Figs. 5(c) and 5(d), respectively. These clearly evidenced that the propagation dynamics of a properly matched probe pulse was dominated by the plasma waveguide and the periodical molecular wakes as observed in our experiments. The plasma column expansion induced waveguide with an axially humped refractive index profile [see Fig. 1(a)(i)] guided the ultrashort laser pulse propagation. An additional cross focusing (or defocusing) effect [see Figs. 1(a)(ii) and 1(a)(iii)], introduced by the pre-aligned neutral molecules in the plasma waveguide with alignment parallel (or perpendicular) to the ultrashort laser pulse polarization, acted as a positive (or negative) lens to strengthen or weaken the guiding effect of the plasma waveguide during the molecular alignment revivals.

IV. CONCLUSION

In conclusion, we have demonstrated that the impulsively aligned neutral molecules significantly influenced the guiding effect of the hydrodynamic plasma waveguide. The time-delayed probe pulse was initially refracted to form a hollow beam by the on-axis laser-induced plasma column and then spatially confined by the hydrodynamic expansion induced plasma waveguide as the time delay increased. The confinement degree of the guided probe pulse could be further modulated with controllable strengthening and weakening when its delay properly matched the molecular quantum wakes.

[1] Y. Ehrlich, A. Zigler, C. Cohen, J. Krall, P. Sprangle, and E. Esarey, Phys. Rev. Lett. **77**, 4186 (1996).

[2] A. Butler, D. J. Spence, and S. M. Hooker, Phys. Rev. Lett. **89**, 185003 (2002).

[3] C. G. Durfee III and H. M. Milchberg, Phys. Rev. Lett. **71**, 2409 (1993); C. G. Durfee III, J. Lynch, and H. M. Milchberg, Phys. Rev. E **51**, 2368 (1995).

[4] V. Kumarappan, K. Y. Kim, and H. M. Milchberg, Phys. Rev. Lett. **94**, 205004 (2005).

[5] For example, A. Couairon, and A. Mysyrowiczb, Phys. Rep. **441**, 47 (2007), and references therein.

[6] J. Yu, D. Mondelain, G. Ange, R. Volk, S. Niedermeier, J.-P. Wolf, J. Kasparian, and R. Sauerbrey, Opt. Lett. **26**, 533 (2001); J. Kasparian *et al.*, Science **301**, 61 (2003).

[7] X. Xie, J. Dai, and X. C. Zhang, Phys. Rev. Lett. **96**, 075005 (2006); Y. Liu, A. Houard, B. Prade, S. Akturk, A. Mysyrowicz, and V. T. Tikhonchuk, *ibid.* **99**, 135002 (2007).

[8] M. Rodriguez *et al.*, Opt. Lett. **27**, 772 (2002).

[9] F. Calegari, C. Vozzi, S. Gasilov, E. Benedetti, G. Sansone, M. Nisoli, S. De Silvestri, and S. Stagira, Phys. Rev. Lett. **100**, 123006 (2008); F. Calegari, C. Vozzi, and S. Stagira, Phys. Rev. A **79**, 023827 (2009).

[10] S. Varma, Y.-H. Chen, and H. M. Milchberg, Phys. Rev. Lett. **101**, 205001 (2008); Phys. Plasmas **16**, 056702 (2009).

[11] J. Wu, H. Cai, H. Zeng, and A. Couairon, Opt. Lett. **33**, 2593 (2008); H. Cai, J. Wu, H. Li, X. Bai, and H. Zeng, Opt. Express **17**, 21060 (2009).

[12] J. Wu, H. Cai, Y. Peng, and H. Zeng, Phys. Rev. A **79**, 041404(R) (2009); H. Cai, J. Wu, Y. Peng, and H. Zeng, Opt. Express **17**, 5822 (2009).

[13] A. C. Bernstein, M. McCormick, G. M. Dyer, J. C. Sanders, and T. Ditmire, Phys. Rev. Lett. **102**, 123902 (2009); J. Wu, Y. Tong, X. Yang, H. Cai, P. Lu, H. Pan, and H. Zeng, Opt. Lett. **34**, 3211 (2009); H. Cai, J. Wu, P. Lu, X. Bai, L. Ding, and H. Zeng, Phys. Rev. A **80**, 051802(R) (2009).

[14] C. G. Durfee III, J. Lynch, and H. M. Milchberg, Opt. Lett. **19**, 1937 (1994); T. R. Clark and H. M. Milchberg, Phys. Rev. E **61**, 1954 (2000).

[15] M. Centurion, Y. Pu, and D. Psaltis, J. Appl. Phys. **100**, 063104 (2006).

[16] J. Kasparian, R. Sauerbrey, and S. L. Chin, Appl. Phys. B**71**, 877 (2000).

[17] M. Spanner, Ph.D. thesis, University of Waterloo, 2004.

[18] V. Renard, M. Renard, S. Guérin, Y. T. Pashayan, B. Lavorel, O. Faucher, and H. R. Jauslin, Phys. Rev. Lett. **90**, 153601 (2003); J. Wu, H. Cai, Y. Tong, and H. Zeng, Opt. Express **17**, 16300 (2009).

[19] J. Wu, H. Cai, A. Couairon, and H. Zeng, Phys. Rev. A **79**, 063812 (2009); **80**, 013828 (2009).